Scripta Materialia 151 (2018) 33–37

Contents lists available at ScienceDirect

Scripta Materialia

journal homepage: www.elsevier.com/locate/scriptamat

Regular article

Special segregation of Cu on the habit plane of lath-like β′ and QP2 precipitates in Al-Mg-Si-Cu alloys

Yaoyao Weng [a,b], Zhihong Jia [a,b,*], Lipeng Ding [a,b], Kui Du [c], Huichao Duan [c], Qing Liu [a,b], Xiaozhi Wu [d]

[a] College of Materials Science and Engineering, Chongqing University, Chongqing 400044, China
[b] Electron Microscopy Center of Chongqing University, Chongqing 400044, China
[c] Shenyang National Laboratory for Materials Science, Institute of Metal Research, Chinese Academy of Sciences, Shenyang 110016, China
[d] College of Physics, Chongqing University, Chongqing 401331, China

ARTICLE INFO

Article history:
Received 28 September 2017
Received in revised form 19 March 2018
Accepted 21 March 2018
Available online xxxx

Keywords:
Al-Mg-Si-Cu alloys
Interfacial segregation
Precipitates
HAADF-STEM
Atomic structure

ABSTRACT

Cu segregation at the habit plane of lath-like β′ and QP2 precipitates for the over-aged Al-Mg-Si-Cu alloys were investigated by atomic resolution high-angle annular dark-field scanning transmission electron microscopy (HAADF-STEM). An even number spacing of Cu segregation (d_{Cu}) was found in the habit plane of the lath-like β′ and QP2 precipitates, which is caused by the strong interaction between the segregated Cu atoms and the Si atoms within the precipitates. The Cu segregation at habit plane of these precipitates can accommodate the lattice misfit that exists between β′ and α-Al matrix.

Segregation of solute atoms at interfaces of metal has received increasing attention in recent years, owing to its significant impact on mechanical properties [1–3]. Solute segregation at phase/matrix interfaces is usually reported to play a critical role in controlling the morphology, performance of phases and consequently influence the microstructure of alloys. For example, Zn segregation at the Mg_2Zn/α-Mg interface can enhance the nucleation of Mg_2Zn phases in Mg-Sn-Zn alloys [2]. Ag and Mg co-segregation at the Ω/α-Al interface greatly stabilize the interface structure and consequently the Ω phases on the $\{111\}_\alpha$ habit planes in Al-Cu-Mg-Ag alloys [4].

Al-Mg-Si(-Cu) alloys are featured by a significant increase in hardness upon aging, which is due to the formation of large numbers of nano-sized metastable precipitates in the α-Al matrix [5–7]. The precipitation sequence of Al-Mg-Si alloys is reported as [5,8]:

SSSS → Atomic clusters → GP zones → β″ → β′, U1, U2, B′ → β, Si.

The needle-like β″ phase responsible for the peak hardness of Al-Mg-Si alloys, and the over-aged β′ (Mg_9Si_5) phase is mainly reported to have rod-shaped morphology. Cu often added to Al-Mg-Si alloys to facilitate precipitation strengthening and improve mechanical property. Cu addition can decrease the precipitation of β″ and result in the formation of Cu containing metastable phases, such as Q′, C phase, during aging treatment. In our recent work, a modified precipitation sequence of Al-Mg-Si-Cu alloys was proposed [9]:

SSSS → Atomic clusters → GP zones → β″, QP1, QP2, C → Q′, QP2, C → Q, Si.

The disordered QP1 and QP2 phases, which contain the unit cell of Q′ and C phase, respectively, are precursor phases of Q′ phase in these alloys. The QP2 phase is similar to the L phase used in many published literatures [10–12] which was proposed as the disordered version of C phase. Due to the absence of clear spots in the diffraction or FFT patterns, the term "L phase" was not used in the present study (detailed explanation about the QP2 phase was described in our previous work [9]). The QP2 can greatly promote aging hardening response and thermal stability of Al-Mg-Si-Cu alloys [13]. Therefore, promoting the preferential precipitation of QP2 phase is expected to improve the properties of Al-Mg-Si-Cu alloy. Solute segregation at phase/matrix interfaces of Al-Mg-Si-Cu alloys has been extensively studied in recent years due to its significant role in controlling the precipitation hardening of these alloys. Saito et al. [14] reported that Cu atoms were generally located at or near the β″/α-Al interface, which could suppress misfit dislocations at the β″/α-Al interface of Al-Mg-Si alloys. Matsuda et al. [15] found Cu segregation at the Q′/α-Al interface in Al-Mg-Si-Cu alloys, which can limit the diffusion growth of Q′ and thus produce finer microstructure. A strong Ag accumulation at the β′/α-Al interface was reported by Marioara et al. [16] in Al-Mg-Si-Ag alloys, where Ag atoms mainly replace the Al on its FCC matrix positions. Wenner et al. [17] investigated the distribution of Cu and Ag atomic columns in the precipitates of Al-

* Corresponding author at: College of Materials Science and Engineering, Chongqing University, Chongqing 400044, China.
E-mail address: zhihongjia@cqu.edu.cn. (Z. Jia).

https://doi.org/10.1016/j.scriptamat.2018.03.032
1359-6462/

Table 1
Compositions of the two investigated Al-Mg-Si-Cu alloys (wt%).

	Mg	Si	Cu	Fe	Mn
Alloy A	1.11	0.67	0.01	0.15	0.06
Alloy B	1.11	0.67	0.5	0.15	0.06

Mg-Si-Cu-Ag alloy by HAADF-STEM and EELS mapping. Cu was observed preferentially along coherent interfaces with the α-Al matrix, and Ag was localized at the narrow ends of precipitates. However, all of these solute segregations were irregularly located at the precipitate/matrix interface, and no segregation was reported in the β′ and QP2 precipitates. In the present study, an atomic-resolution high angle annular dark-field scanning transmission electron microscopy (HAADF-STEM) imaging technique was used to examine the distribution of Cu atoms in the habit plane of lath-like β′, C and QP2 precipitates with α-Al matrix, and the feature of Cu segregation was analyzed and discussed.

Two alloys with different Cu contents were used for the present study. Table 1 shows the compositions of the two investigated Al-Mg-Si-Cu alloys (alloy A and alloy B). These alloys were cast, scalped, homogenized at 560 °C, and then hot and cold rolled to 1 mm thick sheets. Then cold rolled alloys were solution heat treated at 570 °C for 20 min, water quenched and isothermally aged at 170 °C for 3 weeks to obtain the over-aged microstructure. The HAADF-STEM imaging was performed using a spherical aberration probe corrected FEI Titan G2 60–300 TEM, with a Schottky field emitter operated at 300 kV. The probe diameter was 0.08 nm and the collection angle of the HAADF detector was in the range of 45–150 mrad. All HAADF-STEM images shown in this work were taken along the $[001]_{Al}$ direction, corresponding to the precipitate's cross-section. To reduce noise, all the HAADF-STEM images were Fourier filtered with an aperture encompassing all the visible spots in the Fourier transform. Energy dispersive X-ray spectrometry (EDS) data collection in STEM mode uses the 15 mrad collection angle and a spot size 7. The TEM specimens were prepared by electro polishing using a Struers TenuPol-5 machine with the electrolyte consisted of 1/3 HNO_3 in methanol at a temperature between −28 °C and − 30 °C. Geometric phase analysis (GPA) was used to obtain strain fields by applying a cosine mask to $[200]_{Al}$ and $[020]_{Al}$ Fourier spots which provide an accurate way to determine the strain field around phases in α-Al matrix. The theoretical density functional theory (DFT) based studies employed Vanderbilt ultrasoft pseudopotentials as implemented in the plane wave (PW) based code Vienna Ab initio Simulation Package (VASP), with the Perdew–Wang generalized gradient approximation (GGA) for the exchange–correlation energy. All calculations were performed with an energy cut-off of 450 eV and k-point grid of 7 × 7 × 5. For total energy calculations, the electronic relaxation was stopped when the energy difference was less than 10^{-5} eV between two consecutive iteration steps.

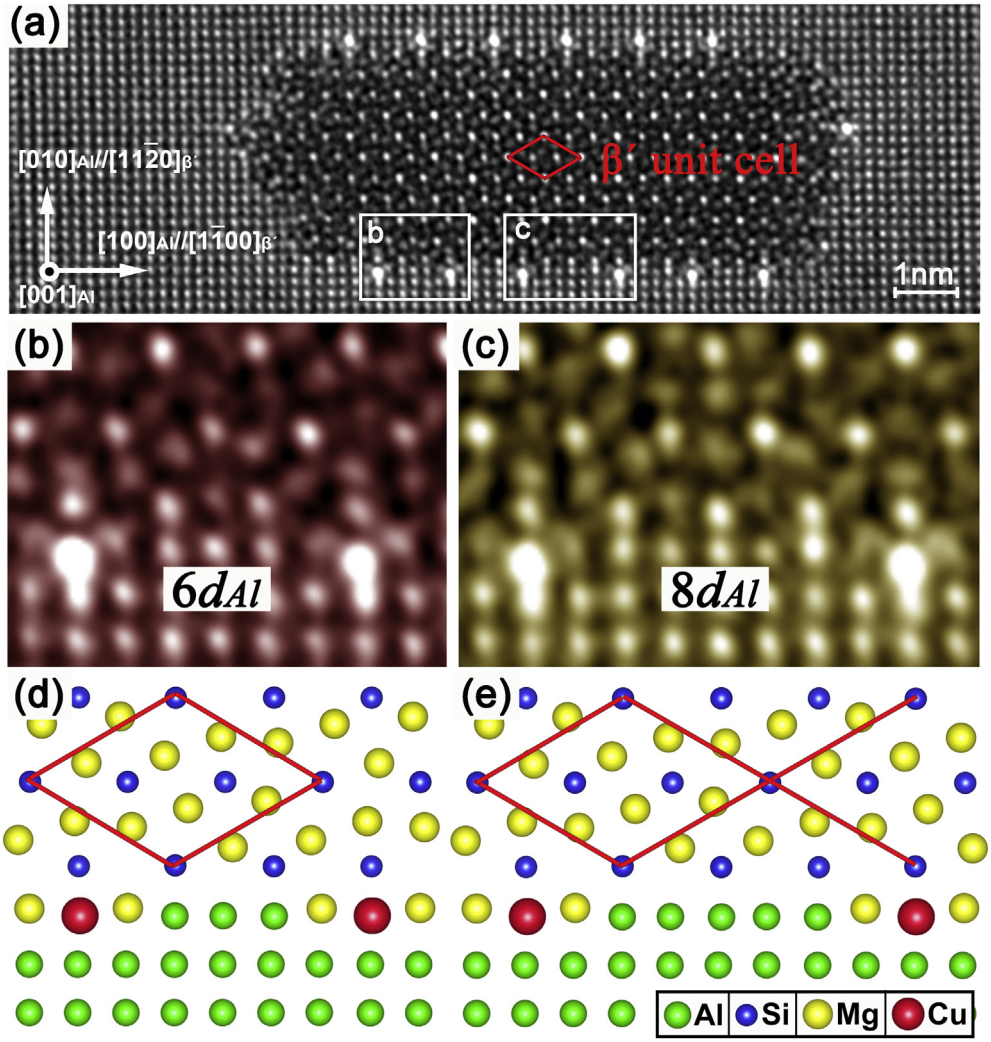

Fig. 1. (a) HAADF-STEM image of cross-section of the lath-like β′ phase, (b) and (c) are the enlarged HAADF-STEM image of the zone b and c marked in (a), respectively. (d) and (e) are corresponding illustration schematic of (b) and (c), respectively. The unit cell of β′ phase is marked by red lines in (a). (For interpretation of the references to colour in this figure legend, the reader is referred to the web version of this article.)